Measurement of the cosmic-ray muon spectrum and charge ratio at large zenith angles in the momentum range 100 GeV/c to 10 TeV/c using a magnet spectrometer

Y. Muraki, Y. Kawashima, T. Kitamura, S. Matsuno, K. Mitsui, S. Miyake, Y. Ohashi, A. Okada, T. Suda, and P. V. Ramana Murthy*
Institute for Cosmic Rays, University of Tokyo, Tanashi, Tokyo 188, Japan

S. Higashi, K. Honda,† S. Ozaki, T. Takahashi, and Y. Teramoto‡
Department of Physics, Osaka City University, Osaka, Japan

Y. Kamiya and I. Nakamura
Department of Physics, Nagoya University, Nagoya, Japan

K. Kobayakawa
Department of Physics, Kobe University, Kobe, Japan

H. Shibata
Department of Physics, Okayama University, Okayama, Japan

Y. Minorikawa
Department of Physics, Kinki University, Higashi Osaka, Japan

S. Mikamo
High Energy Laboratory, Tsukuba-Ohocho, Ibaragi, Japan
(Received 16 September 1981; revised manuscript received 1 March 1983)

The cosmic-ray muon momentum spectrum and charge ratio up to momenta $\simeq$10 TeV/c have been measured with high accuracy. The power index of the differential spectrum of parent mesons at production gradually increases with momentum and becomes 2.84±0.03 in the momentum range 0.8 to 10 TeV/c. The charge ratio is almost constant at a value of 1.27±0.02 from 0.1 to 10 TeV/c.

I. INTRODUCTION

Primary cosmic rays incident at the top of the atmosphere interact with the nuclei of the air and produce pions and kaons. These mesons in turn decay into muons or make nuclear interactions with the air nuclei. The observation of the cosmic-ray muon spectrum and charge ratio yields important information on the hadron-hadron interaction at energies beyond those attainable at the present high-energy accelerators, and on the composition of primary cosmic rays.

The cosmic-ray muon spectrum above 1 TeV has so far obtained only indirectly using the depth-intensity relation of cosmic rays[1] or the muon-produced burst-size spectrum.[2–4] The advantages of using a magnet spectrometer over the other methods are twofold: it is direct and more accurate. The direct observation of the muon spectrum in the past has been restricted to the energy range less than $E_\mu \lesssim 1$ TeV.[5,6]

We have constructed a large magnet spectrometer MUTRON which can measure the muon spectrum and charge ratio between 0.1 and 15 TeV. The spectrometer is located at the Institute for Cosmic Ray Research, University of Tokyo (at sea level) and has been operated for two years. The muon momentum spectrum and the charge ratio have been measured in the zenith-angle range 87° to 90°. In this paper, the detailed results are given; a preliminary report was published earlier.[7]

II. DESCRIPTION OF THE APPARATUS

A schematic view of the MUTRON setup is given in Fig. 1. The magnet spectrometer is composed of two solid-iron magnets each weighing 400 tons, wire spark chambers as the track detector, and muon trigger counters. The trigger counters are located at each side of the magnet spectrometer. In addition, a calorimeter has been located between the two magnets to study muon interactions. The total thickness of the iron calorimeter is

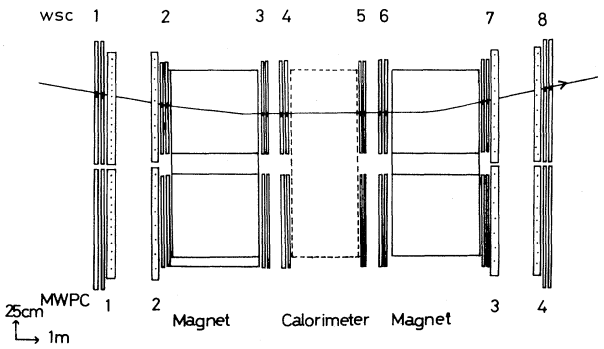

FIG. 1. Schematic view (vertical cross section) of muon spectrometer MUTRON. MWPC and WSC represent multiwire proportional trigger counters and wire spark chambers, respectively (not to scale).

144 cm. The results on interactions induced by the very-high-energy muon have been reported elsewhere.[8] In the following subsections, some details of the various counters are given.

A. Trigger counters

The trigger system is composed of four layers of multiwire proportional counters (MWPC's) and a matrix coincidence system.[9] The adjacent wire distance is 1.2 cm. Each trigger counter covers an area 460×268 cm^2, and two pairs of trigger counters are located in front and at the back of the spectrometer. Muons with momenta higher than 90 GeV/c are selected by the MWPC matrix coincidence system using the 1.2-cm space resolution. The uninteresting low-energy muons are largely deflected away by the magnetic field and are rejected by the hardware logic (the matrix coincidence method). The trigger pulse is created 1.2 μs after the passage of the muons. The overall efficiency of the trigger counter is measured to be 0.95. In order to reduce the background trigger due to air showers, the trigger counters are operated under the following condition: Only the charged particles whose number of associated particles is less than 7 at each MWPC tray are selected.

B. Track detector and data acquisition

The muon position is measured in the x-z projection plane by eight layers of wire spark chambers with magnetostrictive readout, and each layer consists of two gaps.[10] Therefore when all spark gaps fire, 16 points of the projected track location are obtained. Helium gas is circulated inside the spark chamber, and the efficiency of each wire spark chamber is measured to be $\sim$90%.

The position of fiducial points located on each of the chambers is measured by an optical method to an accuracy of $\pm$0.1 mm. Each chamber has two fiducial points attached on the frame of the chamber and one fiducial wire within the 1-cm spark gap. The distance between fiducial point and fiducial wire is measured to an accuracy of $\pm$0.5 mm. Each fiducial wire has been set as horizontally as possible.

After the above procedure, a refined correction of the fiducial wire position has been obtained by software support, by fitting the actual data of a zero-field run to a straight line (by the least-squares method). The position of the fiducial wire is finally adjusted within $\pm$0.1 mm for the four layers of the inside two magnets; for the outer trays the fiducials are adjusted within $\pm$0.3 mm.

The particle-trajectory position in each of the spark chambers is measured by a 10-MHz scaler which is started by the fiducial signal. A maximum of 16 coordinates can be recorded for each channel. The mean propagation speed of the magnetostrictive signal is 1.88 μs/cm. The differences in the magnetostrictive signal speed in the various chambers have also been taken into account. The error in track position due to the electronics coming from the fluctuations in clock frequency and the discrimination level was measured to be $\pm$0.3 mm.[11]

C. Magnet and acceptance

The field of each magnet was measured and the uniformity was found to be $\pm$1%, except for a 100-cm^2 area at each of the four corners of the magnet.[12] There, the field strength deviates by $\pm$2.3% from the standard value. The field strength of the magnet was measured by a flux meter resulting in $\int B\,dl = 64$ kG m.

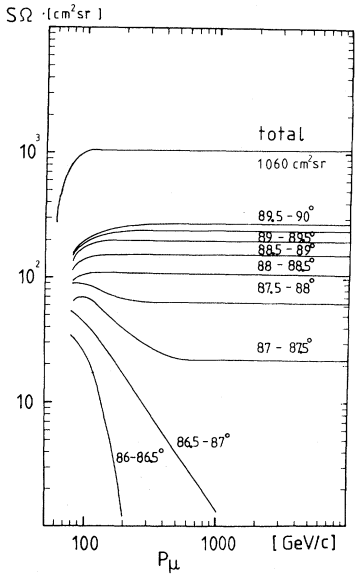

FIG. 2. The total and differential zenith-angle geometrical factors of MUTRON, as a function of muon momentum.

At muon momenta above $p_\mu = 200$ GeV/c, the geometrical acceptance is almost independent of momentum in the zenith-angle range between 87.5° and 90°. The total acceptance (integrated over all the zenith-angle range) of the trigger counter is 1360 cm^2 sr and the net acceptance of the magnet spectrometer is 1060 cm^2 sr. These acceptance dependences on momentum and zenith angle are shown in Fig. 2.

The ratio of the angle of deflection due to the multiple Coulomb scattering to that due to the magnetic field (S/N) is 5%, independent of momentum. Up to momenta $\sim$400 GeV/c, the error in momentum is essentially controlled by this, leading to $\Delta p/p \simeq 0.05$. At higher momenta, spatial resolution errors become more important. The quadratic sum of Coulomb-scattering and spatial-resolution errors leads to $\Delta p/p = 0.08$ at $p_\mu = 1$ TeV/c [at maximum detectable momentum ($p_\mu = 15$ TeV/c),

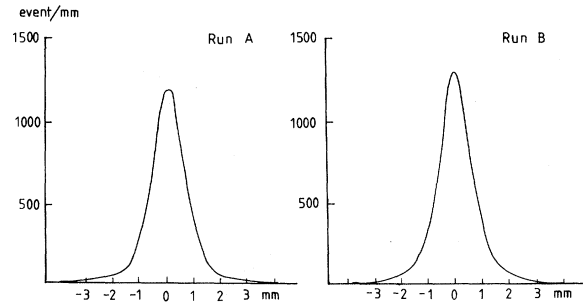

FIG. 3. Spatial resolution of the spectrometer. The data are obtained for the muons with $p_\mu > 800$ GeV/c for runs A and B.

TABLE I. The properties of the muon spectrometer MUTRON.

Location	Tokyo (at sea level)
Angular acceptance ($p_\mu \gtrsim 200$ GeV/c)	87.0°—90.0°
Mean zenith angle	88.8°
Net acceptance ($S\Omega$) ($p_\mu \gtrsim 200$ GeV/c)	1060 m^2 sr
Field strength	16 kG
$\int B\,dl$	64 kG m
S/N ratio ($p_\mu = 400$ GeV/c)	5.0%
S/N ratio ($p_\mu = 1$ TeV/c)	8.0%
Track-chamber-system resolution	0.90 mm
Maximum detectable momentum	15 TeV/c
Trigger efficiency ($p_\mu \gtrsim 200$ GeV/c)	0.95%
Trigger rate	1.05/min

spatial-resolution error equals magnetic deflection by definition; therefore $\Delta p/p = 1$ at $p_\mu = 15$ TeV/c].

D. The maximum momentum detectable by the spectrometer

The maximum detectable momentum (MDM) is an important quantity which determines the sensitivity of the spectrometer. The muon momentum is measured by the bending due to the Lorentz force inside the spectrometer. For example, muons with a momentum of 15 TeV are deflected 0.256 mrad in the magnets and deviate from a straight-line path by 2.6 mm at the opposite-side chamber of the spectrometer.

The MDM is defined as the point where the deflection angle due to the Lorentz force becomes equal to the quadratic sum of the deflection due to the multiple Coulomb scattering and inherent chamber resolution.

As shown in Fig. 3, the spatial resolution of the wire-spark chamber system has the value $\sigma = 0.90$ mm. In this spectrometer 0.90-mm resolution corresponds to a MDM of 15 TeV, when the information from all the 16 spark-chamber gaps is used.

The properties of our spectrometer are summarized in Table I.

III. DATA ANALYSIS

In this section we present some details of the data analysis. The data used in the analysis are listed in Table II.

Since the efficiency of the spark chamber is 90%,[10] not every position of the muon track of the spark gap is always registered. For each event the corresponding momentum resolution which is a function of the number of spark-gap information available (which corresponds to the MDM) has been calculated, and only the events with MDM higher than 11 TeV are used for the present data analysis. The rate is 59% for run A and 44% for run B. In Fig. 4, a typical distribution of MDM for a sample of one run is presented. The difference of the rate between run A and run B comes from the difference of the efficiency of the spark chambers.

The muon momentum is obtained by using the formula of Allkofer *et al.*[13]: The track is approximated to straight lines in field-free regions and to parabolas in the two magnetic-field regions as shown in Fig. 5. The straight lines and the parabolas are connected smoothly at the edges of the magnet.[14] The momentum is obtained by minimizing the χ^2 value for the fitting, as follows:

$$(V)=\sum^{l}\left[a+bz_i+\left[-\frac{L^2}{4}-Lz_i\right]c-x_i\right]^2+\sum^{m}\left[a+bz_i-(L-H)\left[z_i+\frac{L-H}{4}\right]c-x_i\right]^2$$
$$+\sum^{n}\left\{a+bz_i+\left[(2H-L)z_i-\frac{L^2}{4}\right]c-x_i\right\}^2 \qquad (1)$$

and

$$\frac{1}{2}\frac{\partial(V)}{\partial c}=0,\quad p=\frac{300B}{2c\times 10^9}\ \text{GeV}\ .$$

Here x_i and z_i correspond to the vertical and horizontal coordinates; $H/2$ and $L-H$ represent the length of each magnet and the space between the two magnets.

The correct choice of the coordinates that truly correspond to muon trajectory is the most important part for the data analysis. For every combination of the spark

TABLE II. Summary of the data used in the analysis.

	Running period	Total no. of events	High-MDM μ No. of events	Track resolution σ
Run A	30 January 1977—30 September 1977	87 692	51 638 (58.9%)	0.900 mm
Run B	10 May 1978—26 February 1979	109 218	48 462 (44.4%)	0.908 mm

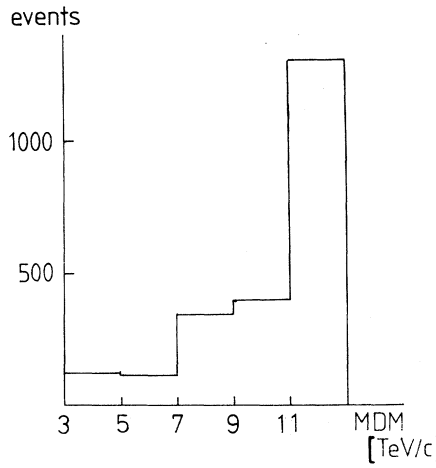

FIG. 4. Typical distribution of MDM for a sample run.

coordinates, a χ^2 test has been made. The events with reduced χ^2 less than 7.3 are regarded as muons. If any spark chamber shows more than one spark, the spark giving the least χ^2 in the fit is chosen as the coordinate of the moun. If any coordinate of one combination deviates over

$$4\times[(0.9)^2+(200/p)^2]^{1/2} \text{ mm}$$

with p in GeV/c, the χ^2 is reexamined after rejection of the coordinate. Here the value $(0.9)^2$ corresponds to the inherent resolution of the spectrometer, and $(200/p)^2$ to the multiple Coulomb scattering. If several solutions exist, the combination which gives the higher momentum resolution has been chosen. When plural solutions yield the same momentum resolution, the event with smallest χ^2 is selected.

Only those muons with the calculated MDM greater than 11 TeV/c have been analyzed further (see Fig. 4). We have checked whether our analysis program has correctly chosen the true muon track or not by having a physicist look at a visual display of the event. We have sampled 1000 trigger events from a typical run and checked the above selection rules on an event-by-event basis and confirmed that the above criterion selects the muon track correctly. No selection failures and no loss of events by selection rules have been found among the 1000 events so examined.

The muon integral spectrum is presented in Fig. 6. The

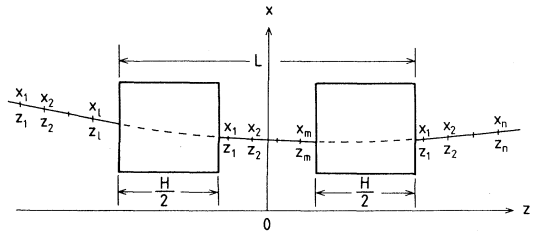

FIG. 5. The muon momentum is obtained by approximating the muon trajectory into separate components comprising straight lines and two parabolas for the magnetic-field regions. l,m,n represent the number of the muon coordinates in each section, and H is the total length of the magnetic region.

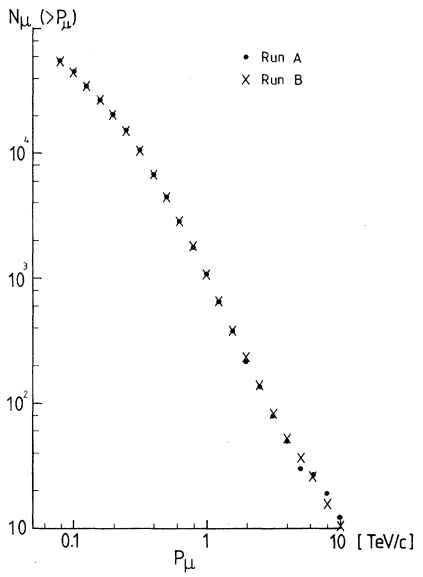

FIG. 6. The muon integral momentum spectrum at sea level for runs A (●) and B (×) from the raw data. The MDM correction has not been made.

solid circles and the crosses in the figure correspond to the runs A and B, respectively. The constants of the alignment have been taken to give the finest resolution of the spectrometer in the respective runs. The agreement between the two data sets suggest that our system is very reliable.

Since our spectrometer does not have a time-of-flight system, the incoming direction could not be identified for the low-energy muons deflected in the upwards direction. However, a muon with energy 1 TeV is bent only by 0.22° by the magnets, and so the incoming direction can be determined for almost all high-energy muons.

Since the cosmic-ray muon spectrum at sea level falls rapidly with momentum as $p_\mu{}^{-3.4}dp_\mu$, the finite resolution of the spectrometer and the multiple Coulomb scattering of muons in the iron cause the low-energy muons to penetrate into the high-energy bins. We must therefore correct this effect in order to obtain the real muon spectrum from the raw data. The correction factor becomes significant in the region near the MDM as shown in Fig. 7.

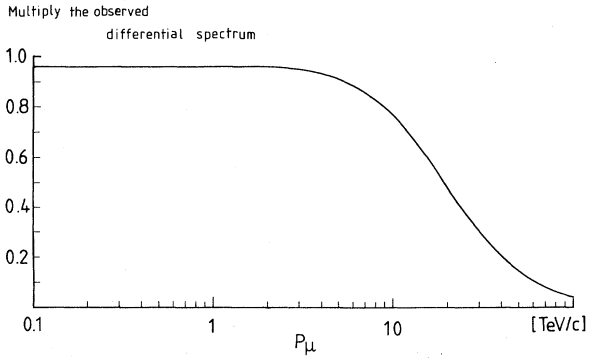

FIG. 7. Multiplicative correction factor for MDM and multiple Coulomb-scattering effects.

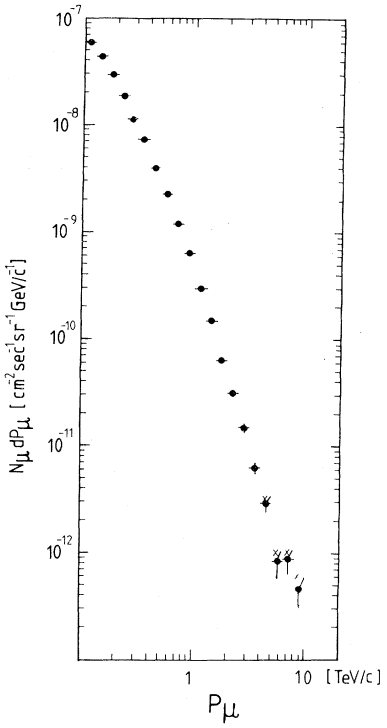

FIG. 8. The muon differential spectrum at sea level. × and ● correspond to the raw and corrected muon differential spectrum, respectively.

The raw and corrected *differential* muon spectra are presented in Fig. 8. The flux values given in Fig. 8 are absolute and not normalized in any way with respect to other data.

As described in Sec. II A, the events whose number of the associated particles is ≥ 7 at each MWPC tray are not selected. Muons passing through the iron magnets associate knock-on electrons or small showers induced by the direct-electron-pair process. The direct-electron-pair production cross section increases with the muon energy and

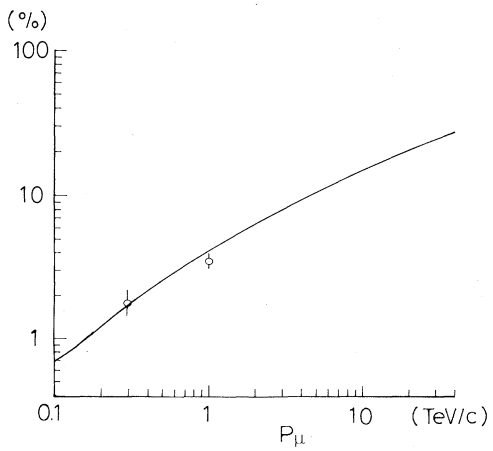

FIG. 9. The rate of the muon rejection by the trigger counter due to the associated particles, as a function of muon momentum. The experimental data points are also given (○).

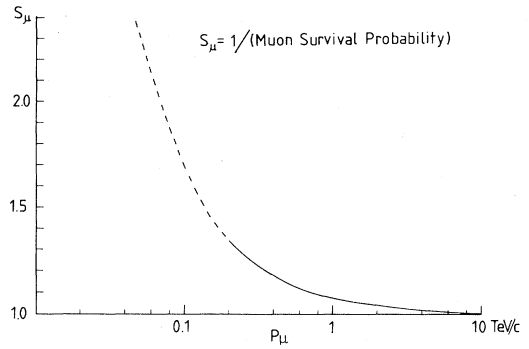

FIG. 10. The multiplicative correction factor S_μ for muon survival probability plotted as a function of the sea-level muon momentum p_μ. The dashed curve is obtained by solving the differential equation by computer.

it gives rise to the momentum dependence of the muon trigger. We have estimated this effect by a full Monte Carlo calculation and compare with present experimental data. The rate of muon loss slowly increases with the muon energy as presented in Fig. 9 and it becomes 4% of the total events at $p_\mu = 1$ TeV/c. For the data analysis, this effect has also been taken account of.

IV. MUON SPECTRUM AT PRODUCTION

In order to compare our present spectrum at sea level with other measurements,[1–4] we transform all data into the muon spectrum at the point of production. The conversion to the production spectrum is done following the standard method.[15]

First the muon momentum at production is obtained by correcting the muon energy loss (ΔE_μ) in the atmosphere from the top to sea level. The energy loss ΔE_μ is evaluated according to Kobayakawa's estimation[16]:

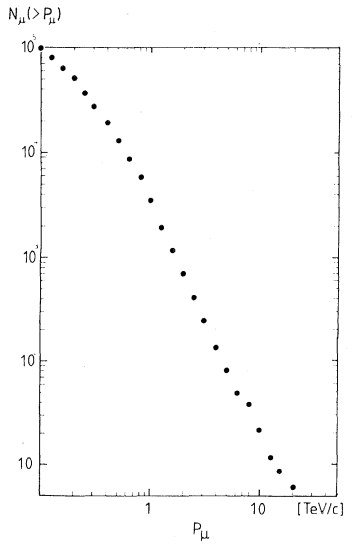

FIG. 11. The muon integral spectrum at production after applying the correction factors.

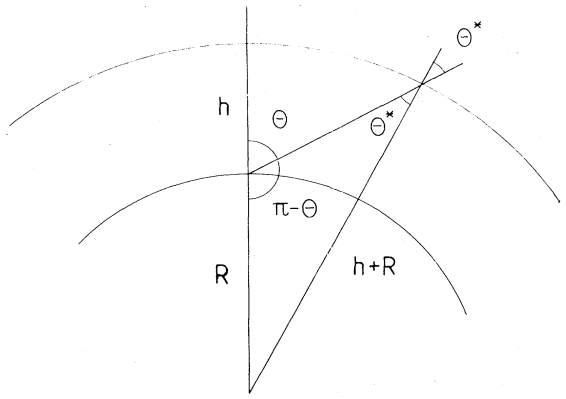

FIG. 12. The relation of the observed zenith angle (θ) of muons to the zenith angle at production at the top of the atmosphere (θ^*).

$$\Delta E_\mu = [(2.5+3.25\times10^{-3}E_\mu)\times10^{-3}X(\theta^*) + 3.15(2.0+8.0\times10^{-3}E_\mu)]\ \text{GeV} . \quad (2)$$

Here E_μ is in GeV. The first term corresponds to the energy loss in the atmosphere, and the second term corresponds to the energy loss inside the magnet; $X(\theta^*)$ refers to the thickness of air expressed in g cm^{-2}.

Since the muon travels a long distance, the correction for the decay loss should also be considered. The multiplicative correction factor S_μ to correct for the muon survival probability is presented in Fig. 10. For the low-momentum muons (less than 200 GeV), the correction factor is obtained by solving the differential equation by computer.[17] The geomagnetic deflection effect should also be taken into account in this calculation. The dashed curve of Fig. 10 is obtained by Kamiya, Shibata, and Iida, based on the above method.

The muon integral number spectrum at production after applying the above corrections is presented in Fig. 11. The mean zenith angle of MUTRON, $\theta=88.8°$, corresponds to $\theta^*=84°$ at the top of the atmosphere: $\sin(\pi-\theta)/(h+R)=\sin\theta^*/R$, where R is the radius of the Earth and h is the production height of the muon as shown in Fig. 12 ($h\simeq32$ km).

In order to obtain the energy spectrum of the parent particles of the muon from the muon spectrum at production, we must define the decay constant. The decay constants of pions (B_π) and kaons (B_K) into mesons are defined as $B_\pi=h_0m_\pi c^2/\tau_\pi c$ and $B_K=h_0m_Kc^2/\tau_kc$: $h_0\simeq6.4$ km (~100 g/cm^2), leading to $B_\pi=114$ GeV, and $B_K=543$ GeV. In the case where pions and kaons travel horizontally at the top of the atmosphere, the probability increases that those mesons decay into muons before they make nuclear interactions. Hence B_π and B_K should be multiplied by secθ^* as illustrated in Fig. 12. In other words, at a deeper zenith angle the decay probability increases according to secθ^* for the same energies E_π and E_K.

The observed muon momentum spectrum $N(E_\mu,\theta)$ can be expressed by the following equation[15]:

$$N(E_\mu,\theta)dE_\mu = AS_\mu E^{-\gamma}\left[r_\pi{}^{\gamma-1}B_\pi\sec\theta^*/(E_\mu+B_\pi\sec\theta^*)+\left[\frac{K}{\pi}\right]r_K{}^{\gamma-1}R_BB_K\sec\theta^*/(E_\mu+B_k\sec\theta^*)\right], \quad (3)$$

where A is the normalization constant, R_B is the $K\to\mu+\nu$ branching ratio, and r_π and r_K refer to the average values of E_μ/E_π and E_μ/E_K in the decays of pions and kaons, respectively. Equation (3) is the first term of the solution of the differential equation which describes the propagation of cosmic rays in the atmosphere. Here we have assumed that charged pion and kaon spectra can be expressed by a simple power law $E_\pi{}^{-\gamma}(E_K{}^{-\gamma})$ with an identical exponent.

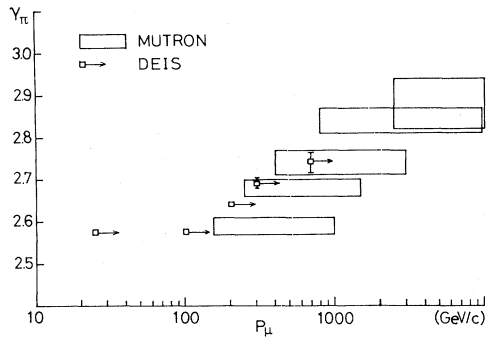

FIG. 13. The power index γ_π of parent mesons. The parent charged pion and kaon spectra have been assumed to be a simple power law $E_\pi{}^{-\gamma_\pi}$. The horizontal limit of the box represents the energy region where χ^2 fitting has been done, while the vertical limit shows the statistical error limit. Recent DEIS data are also plotted.

The K/π ratio is assumed to be 0.15 according to the value of CERN Intersecting Storage Rings (ISR) data.[18] Correct treatment of the large phase-space volume for the kaon in Eq. (3) in relation to that of the pion requires a multiplication factor of 2.4 for the second term of Eq. (3).

The values of γ resulting from the fit to Eq. (3) of differential momentum spectrum of muons at production are presented in Fig. 13 together with other data.[19] It is interesting to note that the parent meson power index γ gradually increases with energy, and it goes to 2.84 ± 0.3 between $E_\mu=0.8$ and 10 TeV (reduced $\chi^2=0.43$). The physical implication of this result is given in Sec. V.

The charge ratio obtained in this experiment is presented in Fig. 14. The charge ratio has an almost constant value of 1.27 ± 0.02 from 0.1 to 4 TeV. The points[20] measured by the Utah group using an indirect method are also plotted together with new data of DEIS,[21] whose MDM is half that of MUTRON. The data point at 7.2 TeV plotted in Fig. 13 has been obtained after MDM correction. The physical implication of the μ^+/μ^- ratio will be discussed in Sec. V.

In closing this section we give the absolute value of the muon spectrum at 1 TeV, which is obtained as follows: The trigger rate (1.05/min) is divided by the trigger efficiency (0.95) and $S\Omega(1360\ \text{cm}^2\,\text{sr})$, and multiplied by the

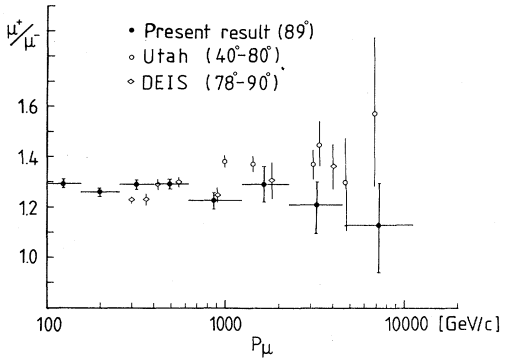

FIG. 14. The muon charge ratio obtained in the present experiment (●) plotted as a function of muon momentum at sea level together with recent DEIS data (◇). Utah points (○) are measured by an indirect method. The MDM of MUTRON and DEIS are 15 and 7 TeV/c, respectively.

percentage of muons within the total events (0.669), and the rate of muons with energy greater than 1 TeV within the total muon rate $(1.69\pm0.06)\times10^{-2}$. The trigger rate (1.05/min) has been already taken account of the live time of the spectrometer system (95%).

The integral muon intensity at $E_\mu \geq 1$ TeV at a mean zenith angle of 88.8° is $(1.53\pm0.15)\times10^{-7}$ cm^2 s^{-1} sr^{-1}. The differential intensity at $E_\mu = 1.15$ TeV is obtained by multiplying by $(8.17\pm0.28)\times10^{-3}$ (the rate of muons with E_μ between 1 and 1.259 TeV) instead of $(1.69\pm0.06)\times10^{-2}$ and dividing by $dE_\mu = 259$ GeV. The result turns out to be $(2.86\pm0.10)\times10^{-10}$ cm^{-2} s^{-1} sr^{-1} (GeV/c)$^{-1}$. This integral and differential intensities at sea level coincide well with the calculation by Murakami *et al.*,[22] within the experimental errors, for $\gamma_{\text{primary}}=2.85$ and $\theta=89°$. The calculation has been based on a Feynman-scaling model and a mixed primary composition ($p/\alpha=26\pm3$/nucleon), and takes account of the rising total cross section. However, the γ_{primary} index 2.85 is ~0.10 higher than the value of the extrapolated primary spectrum ($\gamma_{\text{primary}}=2.75$), obtained by Ryan *et al.*,[23] which fits well with the other muon spectrum for rather-low-energy observations ($E_\mu \leq 1$ TeV).[5,6]

V. RESULTS AND DISCUSSION

Let us compare the γ value obtained by MUTRON with the previous measurements. The γ value in the lower-momentum range $200 < p_\mu < 1000$ GeV/c (2.56 ± 0.016) coincides well with other measurements.[5,6] Our results on γ (2.84 ± 0.03) for the momentum range 1—10 TeV/c are also in agreement, within the stated errors, with the previous results obtained by the horizontal muon emulsion chamber[4] in the momentum range 1—5 TeV/c (2.76 ± 0.12) and in the horizontal-air-shower experiment[3] (2.76 ± 0.20) in the momentum range 2—200 TeV/c. However, the errors in the present results are far smaller than in the results mentioned above. In addition, the DEIS group has also obtained the muon spectrum in the range $0.1 < p_\mu < 7$ TeV/c.[19,21] Their experimental value also confirms our result that the γ value increases with the energies. It becomes 2.74 ± 0.03 in the momentum range 0.8—3.2 TeV/c.

Our result obtained by the direct method, however, gives a larger value of γ (2.84 ± 0.03) than that obtained by the depth-intensity measurement: the vertical muon spectrum can be expressed by the simple power exponent γ (2.66 ± 0.05) in the wide momentum range 0.2—40 TeV/c.[1] In other words, the vertical muon spectrum in the momentum range 1—40 TeV/c can be expressed by the lower value of γ, while the horizontal muon spectrum gradually becomes steeper at ~1 TeV/c.

Since we have published a preliminary result (2.87 ± 0.06),[7] the difference between the horizontal measurement and the vertical observation[1] is a riddle of cosmic-ray muon physics.[24,25] However the correct treatment of the direct production process of the muons from the charmed baryon diffractively produced is made by Halzen[26] and Elbert, Gaisser, and Stanev.[27] They have obtained a result that the muon intensity due to the direct production process becomes of the same intensity as the muons coming from the normal π, K decay at $p_\mu \simeq 10$ TeV/c for the vertical muons and for the horizontal muons it becomes the same for $p_\mu \simeq 70$ TeV/c. This is the reason why our horizontal muon spectrum has a higher γ value than the one for the vertical muons.

Recently the differential hadron-production cross section at $E_{\text{lab}} \simeq 155$ TeV has been obtained by the CERN proton-antiproton collider experiments.[28,29] It is known that Feynman scaling is weakly violated in the central region. However in the very forward region ($x_F \simeq 2p^{\text{c.m.}}/\sqrt{s} > 0.1$), Feynman scaling does work within the experimental errors of 10% in comparison with the cross sections obtained at ISR (2 TeV) and CERN SPS $p\bar{p}$ collider (155 TeV).[30] In other words, even if Feynman scaling is violated, the charged-hadron production cross section at SPS $p\bar{p}$ collider energy is only 10% less than that of ISR energies. This gives rise to an increase of the γ value 0.05 for the muon spectrum in the momentum range 0.5—10 TeV/c. Therefore the high γ value 2.84 obtained by the present experiment cannot be attributed completely to the violation of Feynman scaling. This is the reason why we assert that the primary cosmic-ray flux becomes gradually steeper in the region $E_{\text{primary}} \sim 10$ TeV.

Finally, we mention the calculations on the cosmic-ray muon charge ratio μ^+/μ^-. Frazer *et al.*[31] and Yekutieli[32] have tried to reproduce the observed muon charge ratio using arguments based on the Feynman-scaling model. However, the calculation leads to 1.57 ± 0.10 and is incompatible with our observed value 1.27 ± 0.02.

Taking into account the normal primary compositions, a charge-ratio calculation was recently made.[33] The result indicates that the μ^+/μ^- ratio gradually increases from 1.25 to 1.40 in the momentum range 100 GeV—10 TeV. However the present result indicates a constant charge ratio in the momentum range 1—10 TeV. In the recent ISR experiments,[34] the negative-pion intensity produced by α-α collisions has been obtained. Using the ISR results, we have tried to reproduce the experimental result on the basis of the formulation of Frazer *et al.* and the normal composition of heavy primaries.[35] The value goes down to 1.35, however, still ~0.05 higher than the experimental value. This difference could be explained by introducing an assumption that in the horizontal muon flux at $p_\mu \sim 10$ TeV/c, $\sim10\%$ direct produced muon is included within the muons coming from the normal π-μ decay. The $\sim10\%$ mixture of the direct muons is expected by the cal-

culations of Halzen[26] and Elbert *et al.*[27] This assumption does not contradict with the previous measurement of the zenith-angle distribution of muons for the momentum less than a few TeV/c.[36] More detailed calculation is necessary, taking account of the charmed-baryon and b-flavored-baryon production processes at the very forward region.

We therefore conclude that our experimental result is consistent with the Feynman-scaling model in the very forward region, and the primary cosmic-ray flux, which contributes to muon production, gradually becomes steeper at 10 TeV.

ACKNOWLEDGMENTS

We would like to acknowledge valuable discussions with Professor M.F. Crouch, Professor I. Kondo, Professor H. Muirhead, and Professor V. S. Narashimham. We also express our thanks to the computer center of INS and KEK for providing their facilities.

---

*Present address: Tata Institute for Fundamental Research, Bombay, India.

†Present address: Department of Physics, Yamanashi University, Kofu, Japan.

‡Present address: Brookhaven National Laboratory, Upton, NY 11973.

[1]M. R. Krishnaswamy *et al.*, in *Proceedings of the Fifteenth International Conference on Cosmic Rays, Plovdiv, Bulgaria, 1977,* edited by B. Betev (Bulgarian Academy of Sciences, Sofia, 1977), Vol. 6, p. 85; W. R. Sheldon *et al.*, Phys. Rev. D 17, 114 (1978); M. F. Crouch *et al., ibid.* 18, 2239 (1978).

[2]S. Chin *et al.*, Nuovo Cimento 413, 177 (1971).

[3]M. Nagano *et al.*, J. Phys. Soc. Jpn. 30, 33 (1971); S. Mikamo *et al.*, Lett. Nuovo Cimento 34, 237 (1982).

[4]T. P. Amineva *et al.*, in *Proceedings of the Thirteenth International Conference on Cosmic Rays, Denver, 1973* (Colorado Associated University Press, Boulder, 1973), Vol. 3, p. 1788; K. Mizutani *et al.*, Nuovo Cimento 48A, 429 (1978); M. A. Ivanova *et al.*, in *Sixteenth International Cosmic Ray Conference Kyoto, 1979, Conference Papers* (Institute of Cosmic Ray Research, University of Tokyo, Tokyo, 1979), Vol. 10, p. 35.

[5]S. Iida, Nuovo Cimento 26B, 559 (1975); T. H. Burnett *et al.*, Phys. Rev. Lett. 30, 937 (1975); T. L. Asatiani *et al.*, in *Proceedings of the Fourteenth International Conference on Cosmic Rays, Munich, 1975,* edited by Klaus Pinkau (Max-Planck-Institut, München, 1975), Vol. 6, p. 2024; M. G. Thompson *et al.*, in *Proceedings of the Fifteenth International Conference on Cosmic Rays, Plovdiv, Bulgaria, 1977* (Ref. 1), Vol. 6, p. 21.

[6]R. G. Kellog, H. Kasha, and R. C. Larson, Phys. Rev. D 17, 98 (1978); O. C. Allkofer *et al.*, Phys. Rev. Lett. 41, 832 (1978).

[7]Y. Mukari *et al.*, Phys. Rev. Lett. 43, 974 (1979).

[8]K. Mitsui *et al.*, Nucl. Instrum. Methods 169, 97 (1980); A. Okada *et al.*, Fortschr. Phys. (to be published).

[9]Y. Teramoto *et al.*, Nucl. Instrum. Methods 150, 387 (1978).

[10]Y. Ohashi *et al.*, in *Proceedings of the Fourteenth International Conference on Cosmic Rays, Munich, 1975* (Ref. 5), Vol. 9, p. 3301.

[11]Y. Muraki *et al.*, in *Proceedings of the Fourteenth International Conference on Cosmic Rays, Munich, 1975* (Ref. 5), Vol. 9, p. 3353.

[12]T. Kitamura *et al.*, in *Proceedings of the Thirteenth International Conference on Cosmic Rays, Denver, 1973* (Ref. 4), Vol. 3, p. 1962; K. Mitsui *et al.*, Institute for Cosmic Ray Research, University of Tokyo, Tokyo, Report No. ICR-report-3, 1973) (in Japanese) (unpublished), p. 2.

[13]O. C. Allkofer *et al.*, in *Proceedings of the Twelfth International Conference on Cosmic Rays, Hobart, 1971,* edited by A. G. Fenton and K. B. Fenton (University of Tasmania Press, Hobart, Tasmania, 1971), Vol. 4, p. 1596.

[14]Y. Minorikawa and K. Kobayakawa, Report No. ICR-report-3 (Ref. 12), p. 23.

[15]P. J. Hayman and A. W. Wolfendale, Proc. R. Soc. London 80, 710 (1962); K. Maeda, J. Geophys. Res. 69, 1725 (1964); R. M. Bull, W. F. Nash, and B. C. Rastin, Nuovo Cimento 40A, 365 (1965); O. C. Allkofer, K. Carstensen, and W. D. Dau, Phys. Lett. 36B, 425 (1971).

[16]K. Kobayakawa, in *Proceedings of the Thirteenth International Conference on Cosmic Rays, Denver, 1973* (Ref. 4), Vol. 3, p. 1746.

[17]Y. Kamiya, S. Shibata, and S. Iida, in *Proceedings of the Fifteenth International Conference on Cosmic Rays, Plovdiv, Bulgaria, 1977* (Ref. 1), Vol. 6, p. 32.

[18]A. Bertin *et al.*, Nucl. Phys. B79, 189 (1974); K. Alpgard *et al.*, Phys. Lett. 115B, 65 (1982).

[19]O. C. Allkofer *et al.*, in *Sixteenth Interational Conference on Cosmic Rays, Kyoto, 1979, Conference Papers* (Ref. 4), Vol. 10, p. 56.

[20]G. K. Ashley, II, J. W. Keuffel, and M. O. Larsen, Phys. Rev. D 12, 20 (1975).

[21]O. C. Allkofer *et al.*, in *17th International Cosmic Ray Conference, Paris, 1981, Conference Papers* (Centre d'Études Nucléaires, Saclay, 1981), Vol. 10, p. 321.

[22]K. Murakami *et al.*, in *Proceedings of the Fifteenth International Conference on Cosmic Rays, Plovdiv, Bulgaria, 1977* (Ref. 1), Vol. 6, p. 143.

[23]M. J. Ryan *et al.*, Phys. Rev. Lett. 28, 985 (1972).

[24]Yu. A. Nechin and G. B. Khristiansen, in *Sixteenth International Cosmic Ray Conference, Kyoto, 1979, Conference Papers* (Ref. 4), Vol. 10, p. 146.

[25]M. A. Ivanova *et al.*, in *Sixteenth International Cosmic Ray Conference, Kyoto, 1979, Conference Papers* (Ref. 4), Vol. 10, p. 35.

[26]F. Halzen, in *Proceedings of the 1980 International DUMAND Symposium, Honolulu,* edited by V. J. Stenger (Hawaii DUMAND Center, Honolulu, 1981), Vol. 1, p. 281.

[27]J. W. Elbert, T. K. Gaisser, and T. Stanev, in *Proceedings of the 1980 International DUMAND Symposium, Honolulu* (Ref. 26), Vol. 1, p. 222.

[28]K. Alpgard *et al.*, Phys. Lett. 107B, 310 (1981).

[29]G. Arnison *et al.*, Phys. Lett. 107B, 320 (1981).

[30]J. G. Rushbrook, in *Proceedings of the 21st International Conference on High Energy Physics, Paris, 1982,* edited by P. Petiau and M. Porneuf [J. Phys. (Paris) Colloq. 43, C3-177 (1982)].

[31]W. R. Frazer *et al.*, Phys. Rev. D 5, 1653 (1972).

[32]G. Yekutieli, Nucl. Phys. B47, 621 (1972).

[33]S. A. Stepens, in *Sixteenth International Cosmic Ray Conference, Kyoto, 1979, Conference Papers* (Ref. 4), Vol. 10, p. 96; A. K. Das and A. K. De, *ibid.*, Vol. 10, p. 110; G. Yekutieli, *ibid.*, Vol. 10, p. 123; A. Liland, *ibid.*, Vol. 13, p. 353; Y. Minorikawa and K. Mitsui, in *17th International Cosmic Ray*

Conference, Paris, Conference Papers, 1981 (Ref. 21), Vol. 10, p. 333.

[34]M. A. Faessler, in *Proceedings of the Ninth International Conference on High Energy Physics and Nuclear Physics, Versailles, 1981,* edited by P. Catillon, P. Radvanyi, and M. Porneuf [Nucl. Phys. A374, 461c (1982)].

[35]M. Jacob and Y. Muraki, in *17th International Cosmic Ray Conference, Paris, 1981, Conference Papers* (Ref. 21), Vol. 10, p. 337.

[36]M. R. Krishnaswamy *et al.,* Phys. Lett. 27B, 535 (1968); Institute for Cosmic Ray Research, University of Tokyo, Tokyo, Report No. ICR-report-25, 1975 (unpublished).